iScience

CellPress
OPEN ACCESS

Article

Galectin-8 Enhances T cell Response by Promotion of Antigen Internalization and Processing

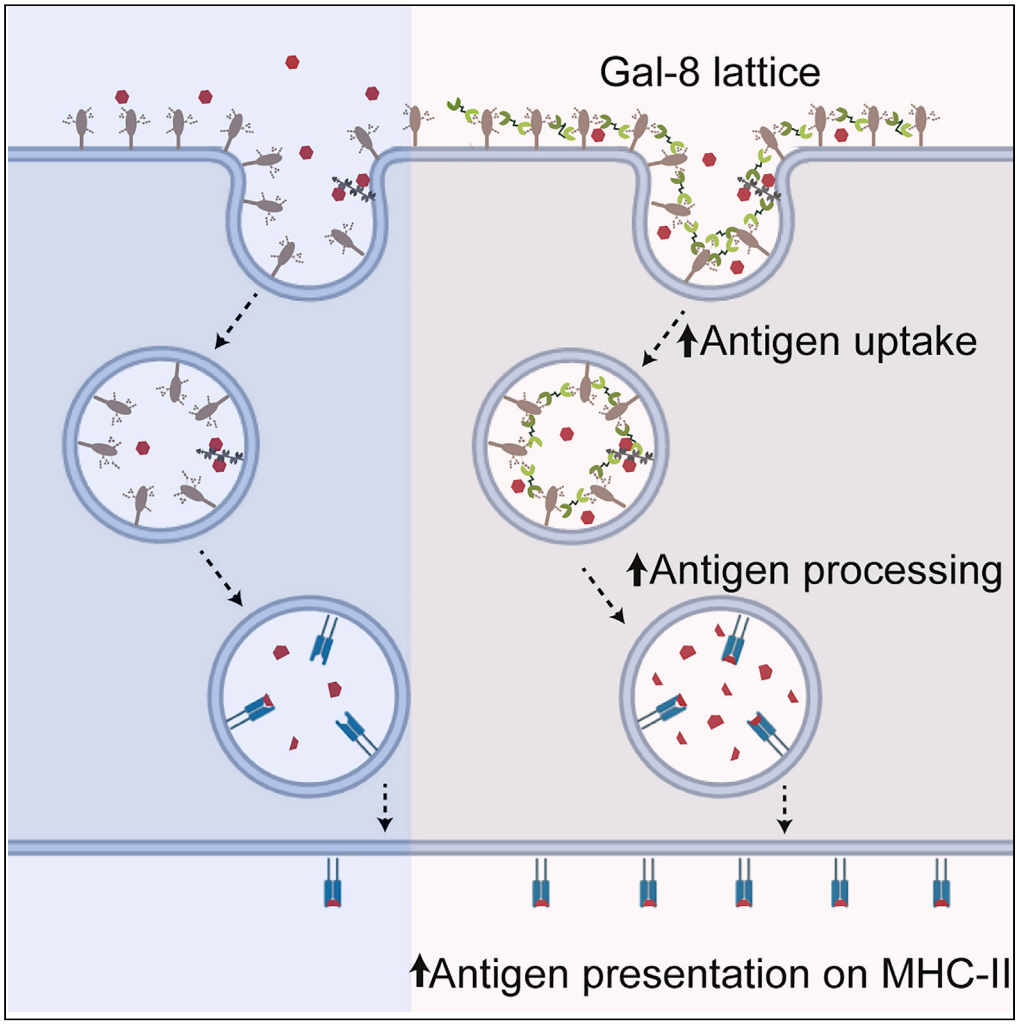

Cecilia Arahí Prato, Julieta Carabelli, Oscar Campetella, María Virginia Tribulatti

vtribulatti@iib.unsam.edu.ar

HIGHLIGHTS

Gal-8-glycan interactions at APC surface induce soluble antigen internalization

Gal-8 and antigen are internalized together in early endosomal compartments

Gal-8 favors antigen proteolytic processing and presentation in the context of MHC-II

Prato et al., iScience *23*, 101278
July 24, 2020
https://doi.org/10.1016/j.isci.2020.101278

iScience

CellPress
OPEN ACCESS

Article

Galectin-8 Enhances T cell Response by Promotion of Antigen Internalization and Processing

Cecilia Arahí Prato,[1] Julieta Carabelli,[1,2] Oscar Campetella,[1] and María Virginia Tribulatti[1,3,*]

SUMMARY

Galectin-8 (Gal-8) is a mammalian lectin endowed with immunostimulatory ability. In the present work, we demonstrate that Gal-8-glycan interactions on the surface of antigen-presenting cells (APCs) promote antigen binding and internalization, independently from antigen nature. Both Gal-8 and antigen were together internalized and localized in early endosomes. Interestingly, antigen processing by APCs was also accelerated in the presence of Gal-8 as a separate mechanism, distinct from the increased antigen internalization. Moreover, APCs pulsed together with antigen and Gal-8 were able to activate cognate $CD4^+$ T cells more efficiently than those pulsed with antigen alone. This enhanced antigen presentation was still evident in the absence of costimulatory signals and APCs-derived soluble mediators. Therefore, our results provide evidence for as yet unrecognized mechanism by which Gal-8 stimulates the elicitation of the immune response in a lectin-dependent manner, by inducing antigen uptake and processing upon lattice formation at APCs surface.

INTRODUCTION

Galectins (Gals) comprise a family of mammalian lectins characterized by the presence of at least one carbohydrate recognition domain (CRD) that binds to *N*-acetyl-lactosamine-containing glycans. By engaging different glycosylated ligands, Gals can mediate multiple cellular functions like adhesion, apoptosis, differentiation, activation, and migration (Elola et al., 2007; Johannes et al., 2018). A particular feature of this family is the building of ordered cell surface Gal-glycan lattices, which induce the aggregation of specific glycoconjugates leading to cell signaling regulation (Brewer, 2002). Gals are synthesized as cytoplasmic proteins to be eventually secreted as soluble factors by a non-classical mechanism. Upon their release, they can bind to glycoproteins and glycolipids present on the cell surface, re-enter the cell by endocytosis, and occupy endocytic and recycling compartments (Johannes et al., 2018; Lepur et al., 2012). Given their particular distribution, Gals can act either intra or extracellularly, thus being involved in diverse cellular processes. Different members of this family have been found in lymphoid tissues, and accumulative evidence has positioned Gals as key mediators of the innate and adaptive immune responses (Liu and Rabinovich, 2010; Martínez Allo et al., 2018).

Galectin-8 (Gal-8), from the tandem-repeat subgroup, is composed of two covalently linked N- and C-terminal CRDs, each displaying different ligand affinity (Stowell et al., 2008). It is expressed in several tissues under normal or pathologic conditions such as inflammation, autoimmunity, and tumors (Elola et al., 2007; Eshkar Sebban et al., 2007; Weinmann et al., 2018). Gal-8 is receiving special attention in terms of its role in the immune system, as its participation in a broad spectrum of functions both stimulating or controlling innate and adaptive responses have been demonstrated (reviewed in Tribulatti et al., 2020). In particular, our group has reported an activating ability during the elicitation of primary antigen-specific responses, postulating Gal-8 as an immunostimulatory molecule (Carabelli et al., 2017; Tribulatti et al., 2009). Among the underlying mechanisms of this stimulatory effect, we found that Gal-8 costimulates *naive* $CD4^+$ T cells in the presence of antigen and antigen-presenting cells (APCs), strengthening TCR signaling, particularly when antigenic signals are weak (Tribulatti et al., 2012). Gal-8 was shown to induce full activation of mouse bone marrow-derived dendritic cells (BMDCs) as well as endogenous splenic dendritic cells (DCs), characterized by an increment of costimulatory molecules, an augmented capacity to activate antigen-specific $CD4^+$ T cell responses, and a strong production of IL-6, among other inflammatory cytokines

[1]Laboratorio de Inmunología Molecular, Instituto de Investigaciones Biotecnológicas, Universidad Nacional de San Martín (UNSAM), Consejo Nacional de Investigaciones Científicas y Técnicas (CONICET), San Martín, Buenos Aires B1650HMP, Argentina

[2]Present address: IrsiCaixa AIDS Research Institute, Barcelona, Spain. Germans Trias i Pujol Research Institute, Barcelona, Spain

[3]Lead Contact

*Correspondence: vtribulatti@iib.unsam.edu.ar

https://doi.org/10.1016/j.isci.2020.101278

(Carabelli et al., 2017). Moreover, we have recently demonstrated that the enhanced levels of IL-6 produced by Gal-8-activated splenic APCs synergize the TCR signaling during antigen presentation to $CD4^+$ T cells, resulting in the Gal-8 costimulatory effect (Carabelli et al., 2018).

DCs are the most efficient APCs endowed with a unique capacity to activate *naive* T cells, and therefore to initiate and direct the adaptive immune response (Steinman, 2006). Immature DCs are localized in peripheral tissues where they efficiently capture antigens through constitutive macropinocytosis, phagocytosis, or receptor-mediated endocytosis. These antigens are further processed into peptides and then loaded onto major histocompatibility complex type II (MHC-II) molecules and presented on the DC surface. When DCs capture antigen in the presence of microbial products or other inflammatory stimuli, they undergo marked morphological and functional changes, called maturation, to optimize antigen presentation to T cells. These changes include an increased migratory capacity to reach lymphoid tissues where T cells reside, acidification of lysosome compartment to promote antigen processing, and up-regulation of costimulatory molecules at DC surface (Mellman and Steinman, 2001; Steinman, 2006). Moreover, it has been described that TLR-induced DC maturation involves an early and transient endocytosis enhancement that can be used to boost antigen capture and presentation (West et al., 2004). In fact, several vaccine adjuvants that induce the activation of adaptative T cell response via DCs were shown to display a direct role in antigen uptake as a mechanism of action (Ahmad et al., 2017; O'Hagan et al., 2012; Reed et al., 2013).

It has been largely reported that different Gals can modulate the uptake of cargo proteins through their interaction with glycoproteins and glycosphingolipids at the cell surface (Furtak et al., 2001; Lakshminarayan et al., 2014; Mathew and Donaldson, 2018; Zappelli et al., 2012). For example, Gal-3 was shown to induce CD44 and β1-integrin internalization, involving the clustering of specific glycoconjugates and the generation of membrane curvature, leading to the formation of tubular endocytic pits (Lakshminarayan et al., 2014). Whether Gals are also able to mediate the internalization of soluble molecules or particles within a functional context is, however, poorly addressed.

Since Gal-8-induced costimulation of specific $CD4^+$ T cell response occurs necessarily in the simultaneous presence of APCs, T cells, and cognate antigen, we propose that Gal-8 can modulate antigen uptake and subsequent processing leading to a more efficient antigen presentation and immune response elicitation. In this study, we analyzed the role of extracellular Gal-8 in antigen internalization, processing, and presentation using BMDCs as model APCs.

RESULTS

Galectin-8 Is Early Internalized by BMDCs in a Glycosylation-Dependent Manner

In the first place, we characterized the internalization of Gal-8 by immature BMDCs, a well-established model for professional phagocytes that are suitable for soluble or particulated antigen uptake. BMDCs were incubated at 37°C in the presence of Alexa 488-Gal-8, and endocytosis was analyzed by confocal microscopy. Gal-8 was early internalized (from 5 min) inside cytoplasmic vesicles, which increased in size along the incubation time (Figure 1A). At the initial time point (0 min), Gal-8 was also found attached to the cell surface, suggesting that Gal-8 first bound to the outer membrane glycoconjugates being readily internalized through active endocytosis. To test this, BMDCs were incubated on ice for 20 min with Alexa 488-Gal-8 in the presence of lactose as a Gal-inhibitor and the binding to the cell surface was analyzed by flow cytometry. The histogram depicted in Figure 1B confirmed that Gal-8 binds to the cell surface in a lectin-glycan-dependent manner since lactose displaced Gal binding. In support, reduced Gal-8 binding to BMDCs surface and subsequent internalization in the presence of lactose was also shown by confocal microscopy (Figure 1C). A fluorescent-labeled mutant Gal-8 (Gal-8mut) that preserves the selective glycan-recognition ability for high-affinity ligands of the *C*-CRD, such as poly-*N*-acetyl-lactosamines and blood group antigens (Schroeder et al., 2016), was similarly endocytosed by BMDCs (Figure 1D). Taken together, these results highlight that Gal-8 is early internalized by BMDCs, involving the recognition of glycans of broad specificity at the cell surface.

Gal-8 Induces Antigen Binding and Uptake by BMDCs

It has been reported that extracellular galectin-glycan interactions play important roles in the endocytosis of different cargo proteins (Lakshminarayan et al., 2014; Mathew and Donaldson, 2018). Considering that Gal-8 is able to stimulate the antigenic response (Carabelli et al., 2017), we hypothesize that Gal-8-built lattices at the cell surface could enhance antigen uptake by DCs, as an additional immunostimulant

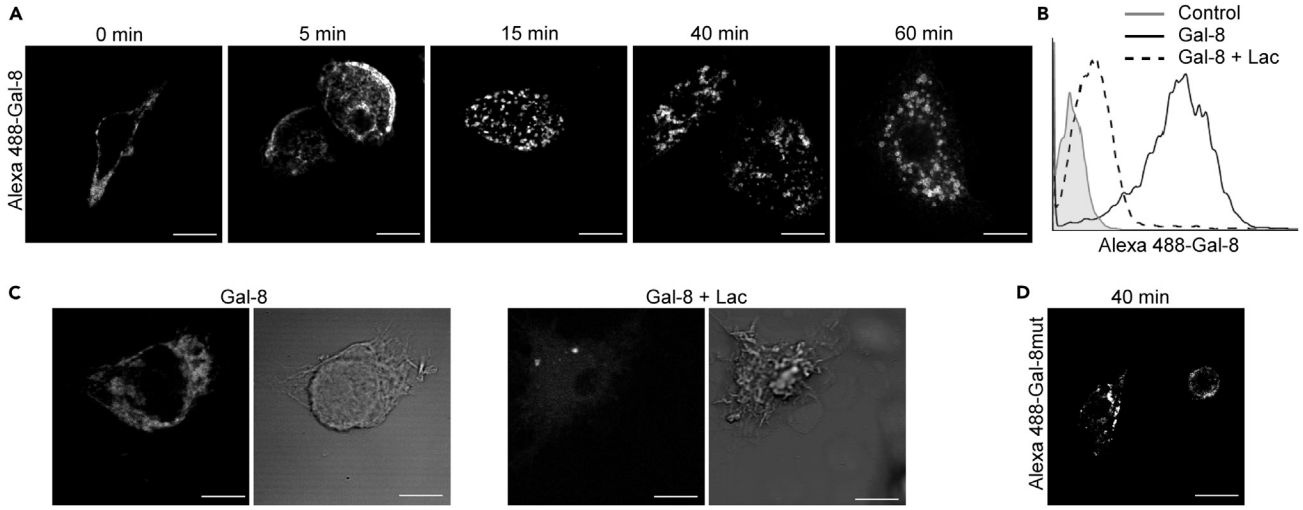

Figure 1. Galectin-8 Is Early Internalized by BMDCs in a Glycosylation-Dependent Manner

(A) BMDCs were incubated with 0.2 μM Alexa 488-Gal-8 on ice (0 min) or at 37°C for 5, 15, 40, and 60 min. Representative confocal microscopy images from each condition are shown. Scale bar: 10 μm.

(B and C) BMDCs were incubated on ice with 0.2 μM Alexa 488-Gal-8 alone (Gal-8) or in combination with 100 mM lactose in 1X PBS (Gal-8 +Lac). Cells without Gal-8 were used as control (B). Cell surface fluorescent signal was analyzed by flow cytometry (B) or confocal microscopy (C). Representative confocal microscopy images are shown. Scale bar: 10 μm.

(D) BMDCs were treated as in (A), except that Alexa 488-Gal-8mut was used. A representative confocal microscopy image is shown. Scale bar: 10 μm.

mechanism. To test this, we used fluorescent-labeled ovalbumin (OVA) as a model antigen. BMDCs were incubated at 37°C in the presence of Alexa 488-OVA together with 2 μM of unlabeled Gal-8 for different time points, and internalization was analyzed by flow cytometry. The selection of Gal-8 concentration used from here on was based on its previously reported ability to induce lattice structures formation (Cattaneo et al., 2011; Tribulatti et al., 2009). As shown in Figure 2A, cells internalized soluble antigen more efficiently when co-incubated with Gal-8 for the periods tested (10 and 45 min). Moreover, when Gal-8-glycan interaction was disrupted with lactose, the increment in antigen internalization was no longer observed, indicating that galectin-glycan interactions were involved in this phenomenon (Figure 2B). When assays were repeated incubating cells on ice instead of at 37°C, no fluorescent signal beyond control cells was observed in OVA-treated cells, confirming that the antigen was internalized by an active endocytic process (Figure 2C). However, OVA fluorescent signal was unexpectedly increased when cells were co-incubated with Gal-8 at low temperature, in a lectin-glycan-dependent manner, suggesting that Gal-8-built lattice is somehow promoting antigen binding at BMDCs surface. In support, the same observation was obtained by confocal microscopy (Figure 2D). The question of whether Gal-8 might be directly interacting with OVA to mediate antigen binding and internalization, either in a lectin-glycan-dependent or -independent manner, arises. However, after many efforts performing OVA-Gal-8 "pull-down" assays as detailed in Methods, we were unable to determine if these proteins are actually interacting (not shown). Therefore, the fact that Gal-8 promotes OVA binding to drive its internalization would not be a consequence of direct interaction between these two proteins, but instead could be intrinsic to Gal-8 interaction with cell surface glycans. At the same time, these findings support the notion that Gal-8 activity may not be specific for OVA protein. Since soluble OVA is internalized by immature APCs mainly by mannose receptor (MR) and pinocytosis (Burgdorf et al., 2007), we wondered whether Gal-8 could induce internalization independently of antigen nature and/or cell surface receptors. To address this, β-casein was selected as a non-glycosylated antigen (Holland, 2008). BMDCs were incubated at 37°C with biotinylated β-casein in the presence of unlabeled Gal-8. After 20 min incubation, internalized β-casein was observed by labeling permeabilized cells with Alexa 488-streptavidin followed by flow cytometry analysis. Remarkably, Gal-8-glycan interaction also induced β-casein endocytosis, indicating that this effect may be independent of the antigen nature and/or the endocytic mechanism (Figure 2E). Internalization indexes of both OVA and β-casein antigens in the presence or absence of Gal-8 are depicted in Figure S1. Interestingly, binding of β-casein to the cell surface was also promoted by Gal-8 (Figure 2F), further highlighting that galectin-glycan interaction permits antigen association at the cell surface, probably representing a required initial step for the Gal-8-induced antigen uptake enhancement. Next, we investigated whether Gal-8 and the antigen follow the same

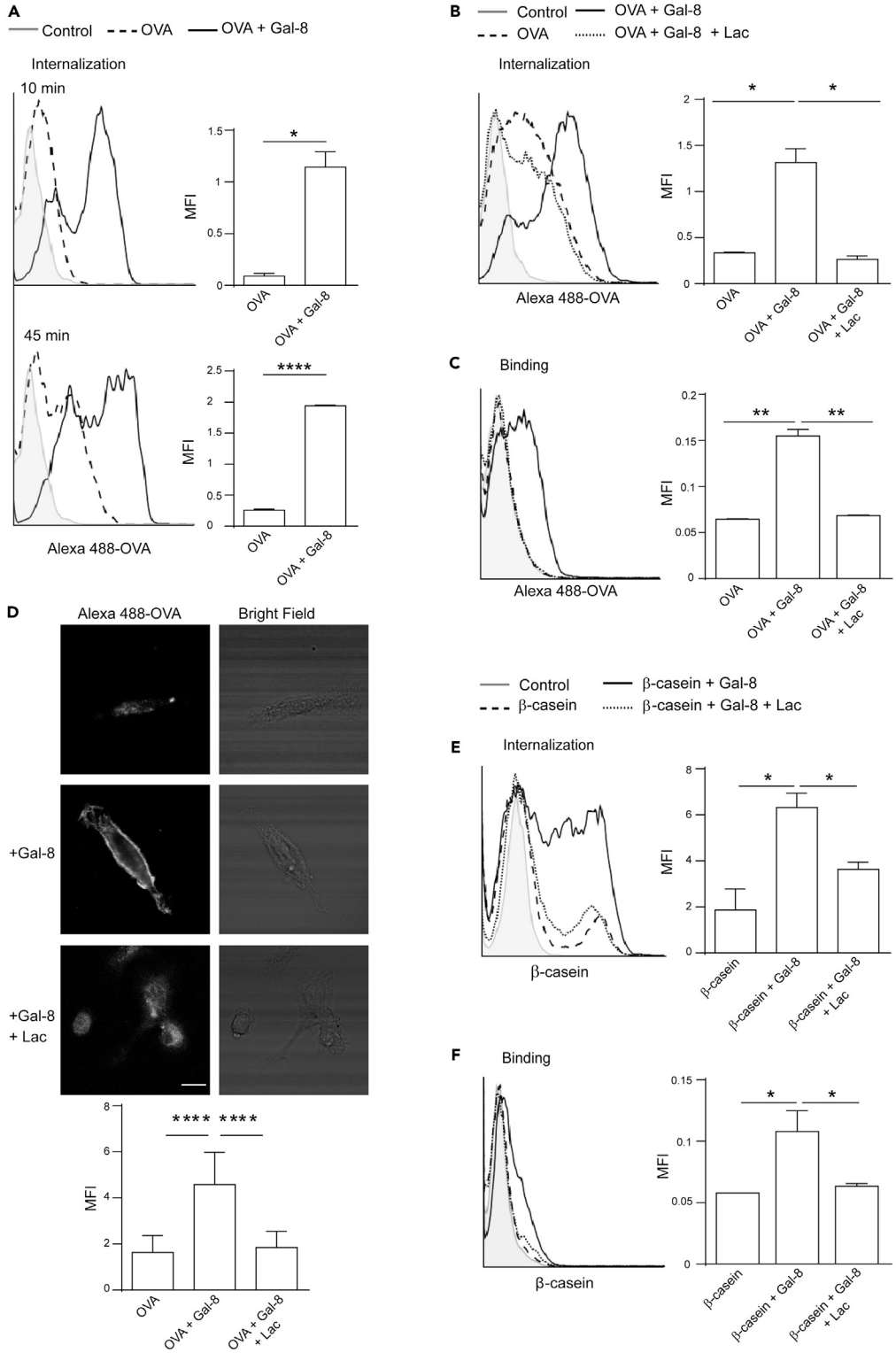

Figure 2. Gal-8 Induces Antigen Binding and Uptake by BMDCs

BMDCs were incubated for the indicated time points with 50 μg/mL Alexa 488-OVA (A–D) or 50 μg/mL biotin-β-casein (E and F) with the simultaneous addition of 2 μM Gal-8; at 37°C for internalization (A, B, and E) or 15 min on ice for cell surface binding (C, D, and F). Where indicated, 100 mM lactose in 1X PBS (Lac) was added together with the stimulus (B - F). For biotin-β-casein detection, cells were fixed and permeabilized before intracellular staining with Alexa

Figure 2. *Continued*

488-streptavidin. The fluorescence signal was analyzed by flow cytometry (A–C, E, and F) or by confocal microscopy (D). Normalized fluorescence intensity of fifteen fields from each condition was registered using FIJI software. Scale bar: 10 μm (D). Bars represent the mean of fluorescence intensity (MFI) ± SD. In all cases, unstimulated cells were used as control. *p < 0.05, **p < 0.01, ****p < 0.0001 (t test). Depicted assays are representative of at least three independent experiments. See also Figure S1.

intracellular route after internalization by analyzing their subcellular localization. BMDCs were incubated simultaneously with Alexa 488-Gal-8 and Alexa 568-OVA at 37°C for 5 and 15 min. Then, cells were washed and fixed, and fluorescence signals were analyzed by confocal microscopy. For longer periods, BMDCs were first pulsed with both fluorescent-labeled stimulus for 15 min, washed, and then chased for another 15, 30, or 60 min at 37°C until cell fixation and microscopic analysis. Notably, a tight association between these two proteins inside cytoplasmic vesicles was readily observed at all the time points tested as shown in Figure 3A, suggesting that Gal-8 is internalized together with the antigen following the same endocytic pathway. Manders' colocalization coefficients for Gal-8 overlapping OVA signal and OVA overlapping Gal-8 signal were calculated. About 60%–85% of both proteins colocalized during all periods tested (Figure 3A). Then, to elucidate the intracellular fate of internalized OVA and Gal-8, the colocalization with different subcellular markers was analyzed. For this purpose, BMDCs were simultaneously incubated at 37°C with Alexa 488-Gal-8 and Alexa 568-OVA for 5, 15, and 20 min or pulsed for 15/20 min and chased for another 15 or 40 min, and then cells were labeled for EEA1, Rab-5, Lamp1, and Rab-7 subcellular markers (Figures 3B and S2). Manders' coefficients for OVA and Gal-8 overlapping with the marker signal were calculated to determine the fraction of each protein on the corresponding compartment. More than 60% of OVA and Gal-8 signal were found inside EEA-1$^+$ and Rab-5$^+$ vesicles at 20 min post exposure, indicating that both proteins were directed to early endosome compartments after internalization (Figure 3B). At longer post-internalization times, OVA and Gal-8 localization in early endosomes decreased as expected, and only a smaller proportion of these proteins (about 45%) were observed inside Rab-7$^+$ or Lamp-1$^+$ vesicles (Figures 3B and S2). The apparent exclusion of Gal-8 and OVA signals from these compartments can be attributable to the fact that antigens are rapidly degraded when they enter the endo-lysosomal pathway in BMDCs. Taken together, these findings demonstrate that OVA antigen and Gal-8 are conjointly internalized by BMDCs and also delineate the intracellular route followed after their endocytosis.

Gal-8 Can Activate Antigen Processing Independently of Uptake

Next, we aimed to investigate whether antigen internalization induced in the presence of Gal-8 affected the subsequent degradation. For this purpose, BMDCs were incubated with Gal-8 and DQ-OVA, a self-quenched conjugate of OVA that exhibits bright fluorescence upon proteolytic degradation, followed by flow cytometry analysis. As depicted in Figure 4A, the presence of Gal-8 resulted in an increased intracellular antigen degradation after 30- and 60-min incubation, confirming that the enhanced OVA signal previously observed in Figures 2A and 2B was not a consequence of reduced or delayed degradation but rather relies upon an augmented internalization rate. Differences in fluorescent signals between DQ-OVA and DQ-OVA + Gal-8 treatments were no longer observed after 2-h incubation (not shown), probably because the probe is reaching a complete degradation at this time as previously reported (Olatunde et al., 2018). Notably, Gal-8-induced degradation was reduced in the presence of lactose indicating that the pro-degradative effect also relied upon lectin-glycan interaction (Figure 4A). Since both stimuli were present in the media during incubation, the augmented DQ-OVA signal induced by Gal-8 could be the result of an accelerated degradation or secondary to an increased internalization. To address this issue, BMDCs were first pulsed with DQ-OVA and Gal-8 for 15 min, washed out, and further incubated for another 15, 45, and 105 min. Histograms depicted in Figure 4B show an increased degradation in cells pulsed in the presence of Gal-8, in agreement with our previous observations. Notably, there was a population of cells pulsed with DQ-OVA plus Gal-8 that displayed a delay in antigen degradation at the earlier time points after the pulse (15 and 45 min). We hypothesized that this population could be "saturated" of antigen due to an augmented internalization induced by Gal-8 during the pulse. However, since BMDCs constitute a heterogeneous group of cells, we cannot discard that these populations respond differently to Gal-8 stimuli. Nevertheless, even assuming that cells had internalized more antigen in the presence of Gal-8, there is another population that exhibited an increased degradation, even at the earliest point (15 min). These observations led us to consider that Gal-8 would be acting by two separate mechanisms: on the one hand by building lattices with cell surface glycoproteins and facilitating antigen internalization/pinocytosis and on the other by intrinsically activating antigen processing. To unequivocally separate these two

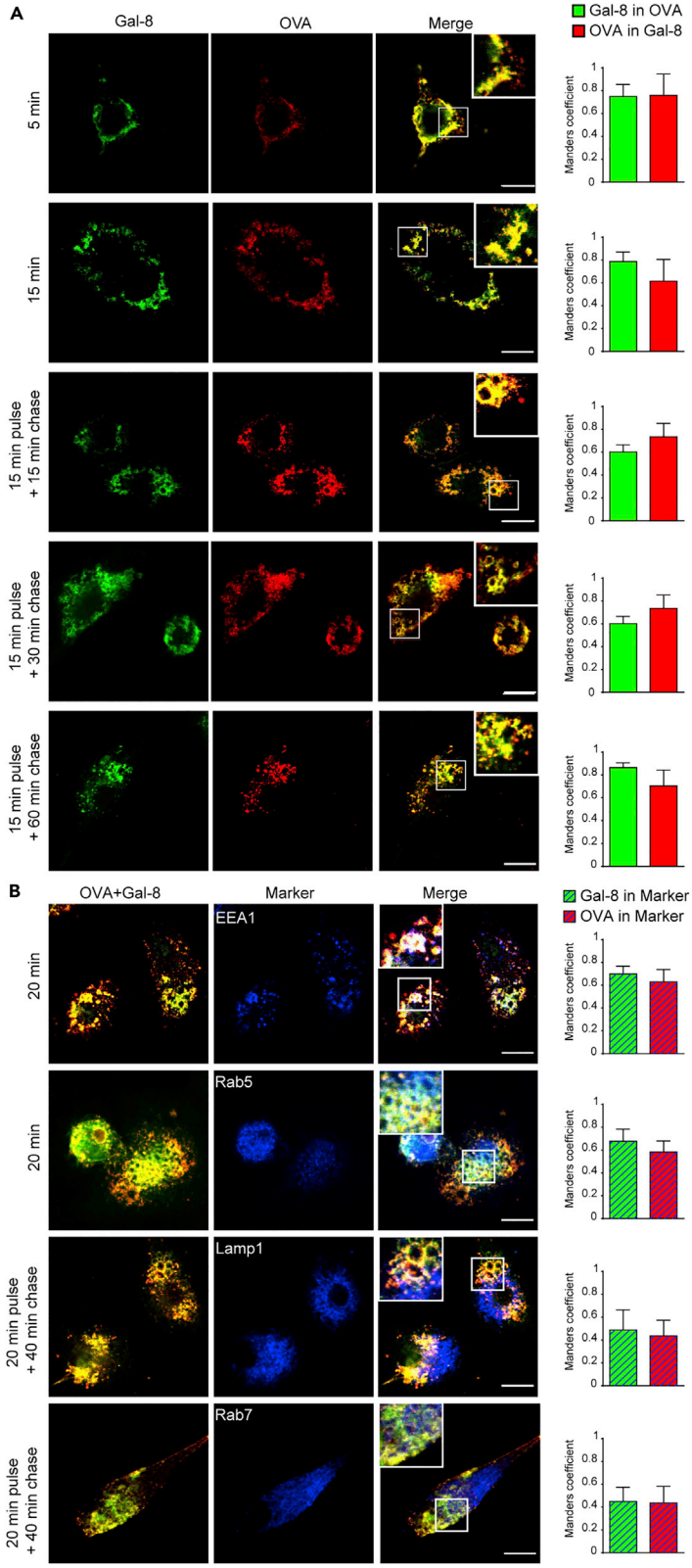
A
Gal-8
OVA
Merge
Gal-8 in OVA
OVA in Gal-8
5 min
15 min
15 min pulse
+ 15 min chase
15 min pulse
+ 30 min chase
15 min pulse
+ 60 min chase
Manders coefficient
B
OVA+Gal-8
Marker
Merge
Gal-8 in Marker
OVA in Marker
EEA1
20 min
Rab5
20 min
Lamp1
20 min pulse
+ 40 min chase
Rab7
20 min pulse
+ 40 min chase

Figure 3. OVA Antigen and Gal-8 Colocalize in the Subcellular Compartments after their Joint Internalization

(A) BMDCs were incubated with 50 μg/mL Alexa 488-OVA and 0.2 μM of Alexa 568-Gal-8 plus 1.8 μM of unlabeled Gal-8 for 5 or 15 min, or were first pulsed during 15 min, washed, and chased for 15, 30, or 60 min. Representative images from confocal microscopy are shown.

(B) BMDCs were treated as in (A) for the indicated time points, then cells were fixed, permeabilized, and stained with anti-EEA1, -Rab5, -Lamp1, and -Rab7. Representative images from confocal microscopy are shown.

Quantification of colocalization of Gal-8 in OVA or Marker signal and colocalization of OVA in Gal-8 or Marker signal was analyzed with Manders' overlap coefficient, which were calculated using the JACOP plugin on FIJI setting the threshold manually. Scale bars:10 μm. Bars represent the mean ± SD of Manders coefficient from 10 fields containing at least two cells per field. See also Figure S2.

mechanisms, we designed an assay that allowed us to demonstrate that both abilities were induced by Gal-8. For this purpose, J774 macrophages were used as APCs, as this cell line is more adequate for this experimental setting. Cells were pulsed for 20 min with DQ-OVA plus biotinylated OVA, washed, and incubated for another 20 min. When Gal-8 was added during the pulse, cells not only internalized more biotin-OVA but also degraded more DQ-OVA, thus confirming that the simultaneous addition of Gal-8 and antigen induced both antigen internalization and proteolytic degradation by immature APCs (Figure 4C). On the other hand, when Gal-8 was added after the mixed antigen pulse, it induced antigen degradation in the absence of further internalization, indicating that antigen degradation induction is independent of its enhanced internalization. Altogether, these findings support an important role for exogenous Gal-8 during antigen uptake and processing and also stress the need for the simultaneous presence of Gal-8 and the antigen to achieve antigen uptake enhancement.

Gal-8 is actively secreted by cells and could remain attached to the surface through interaction with glycoconjugates. To assess whether endogenous Gal-8 may exhibit the ability to induce antigen internalization and processing, assays were repeated with BMDCs obtained from *Lgals8*$^{-/-}$ mice and its C57BL/6J wild-type (WT) counterpart. As observed in Figure 4D, the absence of endogenous Gal-8 did not alter DQ-OVA internalization and/or degradation since no differences in DQ-OVA signal were recorded between *Lgals8*$^{-/-}$ and WT BMDCs. It is conceivable that the presence of other abundant Gals at the cell surface, such as Gal-1 and Gal-3, could counteract Gal-8-induced antigen internalization and processing. Possibly, elevated local amounts of endogenous Gal-8 such as those achieved under inflammatory conditions (which can be recapitulated with exogenous addition of recombinant protein) are needed to effectively build a lattice and further counteract the effect of other Gals-formed lattices. In fact, when recombinant Gal-8 was added in combination with DQ-OVA, the increased fluorescence signal was likewise observed in both Gal-8-deficient and WT cells (Figure 4D), further indicating that the exogenous Gal-8 is sufficient to induce antigen internalization and degradation.

BMDCs Pulsed with OVA and Gal-8 Present Antigen More Efficiently

After being internalized by APCs, antigens are directed to lysosomal compartments where they are processed to originate peptides that accommodate onto molecules, to be presented to cognate T cells. Therefore, we asked whether the increased antigen internalization and processing in the presence of Gal-8 was traduced in a more efficient recognition and activation of specific T cells. When *naive* CD4$^+$ T cells purified from TCR_{OVA} transgenic OT-II mice were cultured in the presence of BMDCs previously pulsed for 45 min with OVA and Gal-8, a significant increased T cell proliferation and IFN-γ secretion were recorded, compared with cells pulsed with OVA only (Figure 5A). Remarkably, when this assay was repeated using the cognate OVA peptide ($OVA_{323-339}$) instead of the whole protein, no differences in T cell activation were registered when the pulse was performed either in the presence or absence of Gal-8 (Figure 5A). The latter strongly suggests that the enhanced T cell activation was a result of a greater antigen presentation by BMDCs that had internalized and processed more OVA in the presence of Gal-8. To confirm that Gal-8 was increasing antigen presentation to T cells, independently from its previously reported activating effect on APCs (Carabelli et al., 2017), we repeated the assay depicted in Figure 5A, but in this case BMDCs were fixed with glutaraldehyde after the pulse. As shown in Figure 5B, fixed BMDCs previously pulsed in the presence of Gal-8, induced a more efficient antigen presentation to T cells, even when costimulatory signals and APCs-derived soluble factors were not involved. This result indicates that Gal-8-pulsed BMDCs display increased levels of MHC-II-antigen complexes at the surface. We have previously demonstrated that Gal-8 activates APCs to produce IL-6 during antigen presentation and that interleukin signaling is involved in the Gal-8-induced elicitation of CD4$^+$ T cell antigenic response (Carabelli et al., 2018). Given that IL-6 was demonstrated to positively regulate cathepsin S expression in DCs (Kim et al.,

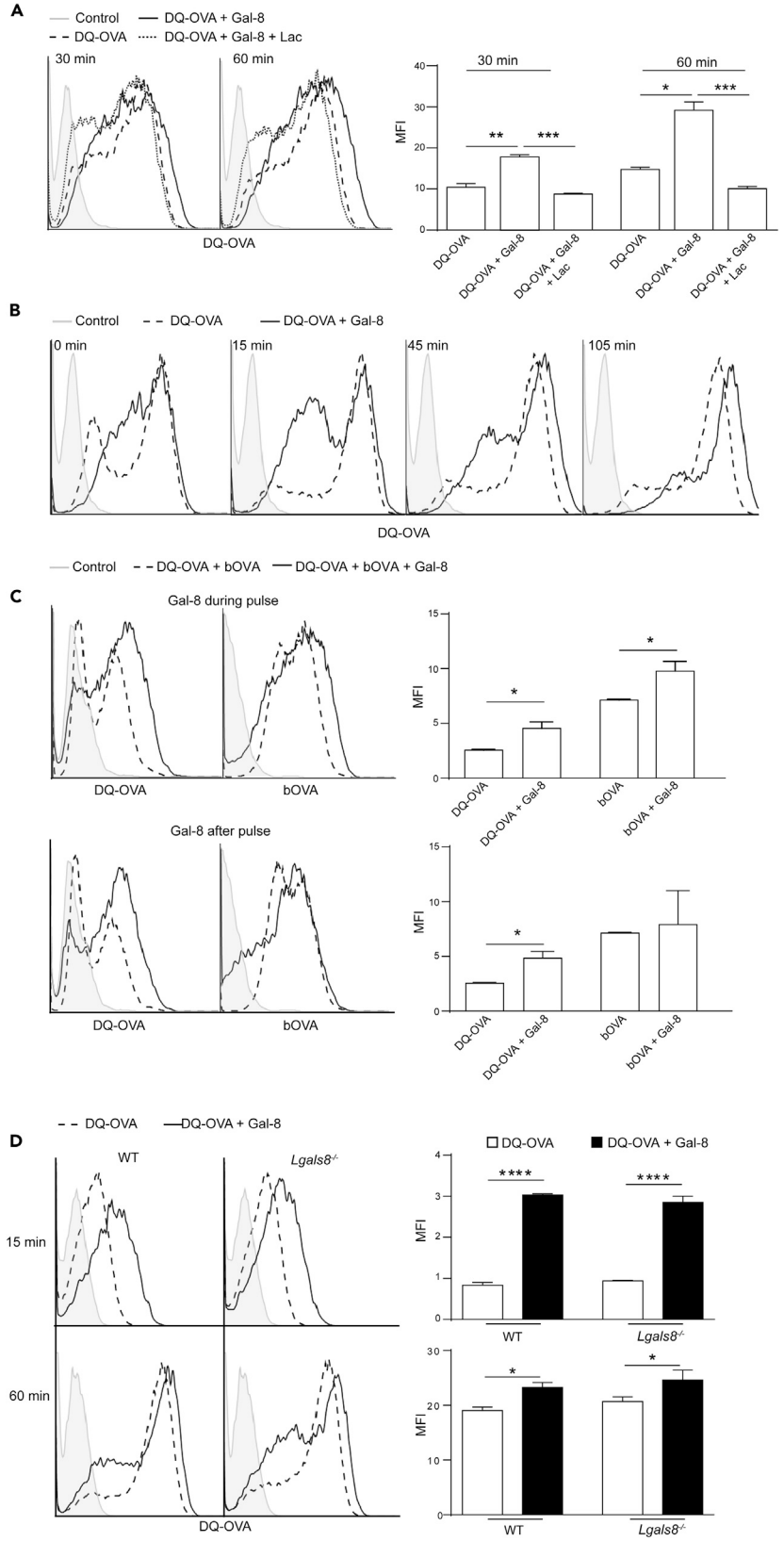
A
Control
DQ-OVA
DQ-OVA + Gal-8
DQ-OVA + Gal-8 + Lac
30 min
60 min
DQ-OVA
MFI
30 min
60 min
**
***
*
***
DQ-OVA
DQ-OVA + Gal-8
DQ-OVA + Gal-8 + Lac
B
Control
DQ-OVA
DQ-OVA + Gal-8
0 min
15 min
45 min
105 min
DQ-OVA
Control
DQ-OVA + bOVA
DQ-OVA + bOVA + Gal-8
C
Gal-8 during pulse
DQ-OVA
bOVA
MFI
*
*
DQ-OVA
DQ-OVA + Gal-8
bOVA
bOVA + Gal-8
Gal-8 after pulse
DQ-OVA
bOVA
MFI
*
DQ-OVA
DQ-OVA + Gal-8
bOVA
bOVA + Gal-8
D
DQ-OVA
DQ-OVA + Gal-8
WT
Lgals8-/-
15 min
60 min
DQ-OVA
DQ-OVA + Gal-8
MFI
****
****
WT
Lgals8-/-
MFI
*
*
WT
Lgals8-/-

Figure 4. Gal-8 Can Activate Antigen Processing Independently of Uptake

(A) BMDCs were incubated with 50 μg/mL DQ-OVA for 30 or 60 min at 37°C in the presence of 2 μM Gal-8, with or without 100 mM lactose in 1X PBS (Lac).

(B) BMDCs were pulsed with 50 μg/mL DQ-OVA together with 2 μM Gal-8 for 15 min at 37°C. Then cells were washed and chased for the indicated times.

(C) BMDCs were pulsed with 50 μg/mL DQ-OVA and 50 μg/mL biotin-OVA (bOVA) for 20 min at 37°C in the presence (top) or absence (bottom) of 2 μM Gal-8. Then, cells were washed and incubated for another 20 min at 37°C in the presence (bottom) or absence (top) of 2 μM Gal-8. For biotin-OVA detection, cells were fixed and permeabilized before intracellular staining with PE-Cy5-streptavidin.

(D) BMDCs differentiated from *Lgals8*$^{-/-}$ or C57BL/6J (WT) mice were pulsed with 50 μg/mL DQ-OVA together with 2 μM Gal-8 for 15 or 60 min at 37°C.

Fluorescence emitted by the hydrolyzed DQ-OVA probe and PE-Cy5-streptavidin was analyzed by flow cytometry. Bars represent the mean of fluorescence intensity (MFI) ± SD. In all cases, unstimulated cells were used as control. *$p < 0.05$, **$p < 0.01$, ***$p < 0.001$(A and C, t test). *$p < 0.05$, ****$p < 0.0001$ (D, ANOVA). Depicted assays are representative of at least three independent experiments.

2017), we wondered whether this cytokine could be participating in Gal-8-induced antigen processing. To answer this question, BMDCs were differentiated from *Il6*$^{-/-}$ mice (*Il6*$^{-/-}$ BMDCs) or C57BL/6J control mice (WT BMDCs) and pulsed with DQ-OVA and Gal-8. Both IL-6-deficient and WT BMDCs showed increased antigen proteolysis in the presence of Gal-8, indicating that IL-6 signaling does not participate in Gal-8-induced antigen processing (Figure S3A). Moreover, no differences were observed between the antigen-presentation ability of fixed IL-6-deficient and WT BMDCs pulsed in the presence of Gal-8, thus disregarding any effect of IL-6 signaling in Gal-8-induced internalization and processing (Figure S3B).

Taken together, our results provide supporting evidence that Gal-8 is able to induce binding, internalization, and processing of soluble antigens by APCs, to increment presentation to specific CD4$^+$ T cells, as an additional mechanism of its immunostimulatory effect.

DISCUSSION

The Gals-glycan interaction is a complex field that is in continuous development. Here, we demonstrated that Gal-8-glycan interaction at the cell surface can modify soluble antigen internalization by APCs, a crucial step in the elicitation of a given immune response. It has been previously shown that Gal-8 binding to cell surface glycans constitutes an initial requirement for its subsequent internalization by a non-clathrin, non-caveolae-mediated mechanism in different cell lines (Carlsson et al., 2007). In agreement, we observed that soluble Gal-8 is early internalized by BMDCs on a lectin-glycan-dependent manner since lactose treatment diminishes both Gal binding and endocytosis. Given its particular "heterodimeric" structure with two distinct CRDs organized in tandem, Gal-8 can recognize ligands within a wide affinity range (Stowell et al., 2008). Our mutant version of Gal-8 (Gal-8 mut), which only recognizes high-affinity ligands such as poly-*N*-lactosamines and blood group antigens (Schroeder et al., 2016), similarly bound and entered BMDCs. Since lactose only displaces the intermediate- and low-affinity (second best) ligands, our results suggest that Gal-8 first binds with broad specificity to *N*-linked glycans at the BMDC surface prior to its internalization and traffic along the endocytic compartments.

Changes in cell surface glycosylation and Gal expression appears to tailor lattice formation, further modifying membrane dynamics (Mathew and Donaldson, 2019). Gal-built lattices were shown to modulate clathrin-independent endocytosis of different glycosylated cargo proteins. Lakshminarayan et al. (2014) demonstrated that Gal-3 binding to CD44 and α5β1 integrin triggers Gal oligomerization and its interaction with glycosphingolipids to generate membrane curvature, finally leading to the formation of endocytic "pits." On the other hand, Mathew and Donaldson (2018) reported that Gal-3 can stimulate or counteract the internalization of CD59 and MHC-I molecules depending on the strength of glycan interaction, lattice extension, and cell type. In this context, it is reasonable to pose that Gal-8 with two active CRDs with different glycan specificity could alter membrane fluidity by building a particular arrangement with glycoconjugates when exogenously added. In fact, it has been reported very recently that extracellular Gal-8 drives endophilin-A3-dependent endocytosis of CD166, through its interaction with glycolipids located at the cell membrane (Renard et al., 2020). In this work, we provide evidence that Gal-8-built lattice can induce soluble antigen internalization by APCs. Interestingly, soluble antigens seem to be retained or trapped on the outer membrane upon Gal-8-glycan interaction before their uptake by APCs. This initial effect may constitute the first step for the enhanced antigen internalization. DCs can internalize OVA antigen by mannose receptor as well as macropinocytosis (Burgdorf et al., 2007). It is possible that, upon lattice formation, the

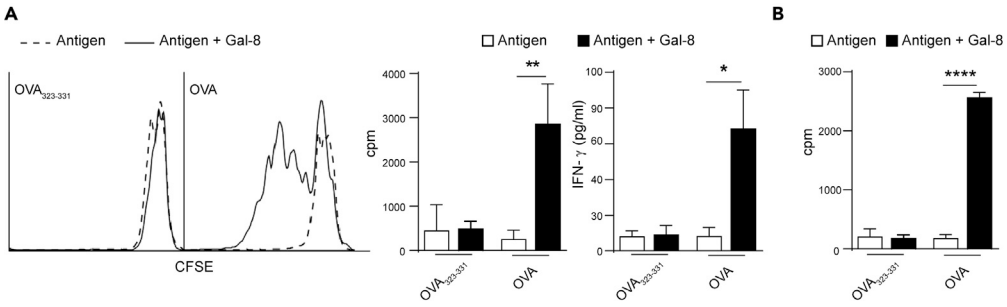

Figure 5. BMDCs Pulsed with OVA and Gal-8 Present Antigen More Efficiently

(A) BMDCs were pulsed with 0.1 μg/mL OVA peptide ($OVA_{323-339}$) or 500 μg/mL OVA protein (OVA) in the presence of 2 μM Gal-8 for 45 min at 37°C, and then, cells were washed and co-cultured with $CD4^+$ T cells purified from OT-II mice splenocytes. Cell proliferation was determined after 72 h by [^{3}H]-methylthymidine incorporation (right) or after 6 days by CFSE dilution and flow cytometry analysis (left). IFN-γ secretion was analyzed in supernatants from 6 days BMDC:$CD4^+$ T cell co-cultures by ELISA.

(B) BMDCs were pulsed with 0.1 μg/mL OVA peptide ($OVA_{323-339}$) or 1 mg/mL OVA protein (OVA) in the presence of 2 μM Gal-8 ON at 37°C. Then, cells were washed, fixed, and co-incubated with $CD4^+$ T cells purified from OT-II mice splenocytes. After 72 h of culture, cell proliferation was determined by [^{3}H]-methylthymidine incorporation.

*$p < 0.05$, **$p < 0.01$, ****$p < 0,0001$, (*t* test). cpm: counts per minute. Bars represent the mean ± SD. Depicted assays are representative of at least four independent experiments. See also Figure S3.

scavengers and lectin-like receptors present in DC surface may display an increased avidity for their antigens. Macropinocytosis, a type of clathrin-independent endocytosis, was also shown to be affected by changes in membrane dynamics induced by Gal-lattices (Mathew and Donaldson, 2018). On the other hand, it was previously shown that soluble Gal-8 or Gal-8 as a matrix component binds to cell surface integrins to induce PI3K-, Rac-1-, and ERK-dependent actin cytoskeletal rearrangements leading to cell spreading and lamellipodial extensions in several cell types (Cárcamo et al., 2006; Levy et al., 2001). In line with this, we observed that BMDCs cultured in the presence of Gal-8 display a mature phenotype characterized by cell spreading and dendrites prolongation (Carabelli et al., 2017). Since actin remodeling was shown to be involved in antigen pinocytosis of newly activated DCs (West et al., 2004), it is conceivable to pose that Gal-8-induced cell spreading could also participate in antigen uptake enhancement. In support of our findings, Obino et al. (2018) have reported that exposure of specific B cells to particulate-antigen coated with Gal-8 increased their internalization capacity *in vivo*, reinforcing a role for extracellular Gal-8 in favoring the phagocytosis process as well.

Since we observed that OVA entered the cells in the same compartments as Gal-8 when offered together (Figure 3A), we speculated that Gal-8 could be interacting with OVA (most probably in a lectin-glycan dependent manner), thus explaining the increased antigen binding and uptake. However, after many efforts performing OVA-Gal-8 pull-down assays, we were unable to demonstrate that these two proteins were actually interacting, either by lectin-glycan or protein-protein manner. This outcome was not entirely unexpected since OVA is highly decorated with mannose, a sugar that is not recognized by Gal-8 (Schroeder et al., 2016). Moreover, the non-glycosylated β-casein binding and uptake in APCs were also increased in the presence of Gal-8, thus widening the spectrum of antigen nature and internalization mechanism for this Gal-8 effect. Therefore, our findings strengthen the notion that antigen binding and endocytosis induction result from membrane modifications induced by Gal-8-lattice formed with cellular surface glycans, rather than a direct interaction between antigen and Gal-8.

In this work, we found that both Gal-8 and OVA were mainly localized in early endosomes soon after their internalization and practically excluded from the lysosomal compartments (Figure 3). The efficient proteolytic activity for the delivered antigens in BMDCs could account for the apparent absence of these proteins in the degradative compartments. In agreement, other authors failed to detect OVA inside Rab-7^+ or $Lamp1^+$ vesicles in BMDCs (Burgdorf et al., 2007; Franken et al., 2013). Moreover, Coria et al. (2016) were only able to trace OVA antigen inside the $Lamp2^+$ lysosomal compartment when BMDCs were co-delivered with a protease inhibitor. Nevertheless, the joint internalization of Gal-8 and antigen did not affect the subsequent processing, as the DQ-OVA substrate was degraded (Figure 4) and antigen-driven CD4 T^+ cell activation was readily observed (Figure 5). On the other hand, it is already known that, according to the uptake mechanism, the antigen can follow different pathways that will ultimately determine whether it is presented on MHC-I or MHC-II molecules

(Burgdorf et al., 2007). Soluble antigens intended for classical exogenous MHC-II-restricted presentation are routed into lysosomes, whereas those destined for cross-presentation are maintained in stable early endosomes (Burgdorf and Kurts, 2008; Lutz et al., 1997). Although the present work is focused on Gal-8-induced $CD4^+$ T cell response, we cannot discard that the antigen could be also following a cross-presentation route since soluble OVA can be presented to both $CD4^+$ and $CD8^+$ T cells.

Both fluid-phase and receptor-mediated endocytic pathways rely on intracellular processing followed by loading onto MHC-II molecules. Here, we observed that Gal-8-stimulated BMDCs and J774 macrophage cell line display a major antigen processing ability not only as a consequence of an augmented internalization but also due to an increased proteolysis rate. IL-6 signaling, which is involved in the Gal-8-induced elicitation of $CD4^+$ T cell antigenic response (Carabelli et al., 2018), was also shown to positively regulate cathepsin S expression in DCs (Kim et al., 2017). However, *Il6*$^{-/-}$ and WT BMDCs showed similar antigen proteolysis in the presence of Gal-8, thus disregarding IL-6 signaling participation in Gal-8-induced antigen processing. Considering that an increased fluorescent signal from degraded DQ-OVA implies more molecules being processed, Gal-8 could be promoting antigen degradation by modifying the traffic rate in BMDC leading to an increased amount of antigen presented on the MHC-II context. Nevertheless, the exact mechanism by which Gal-8 induces antigen degradation remains to be addressed.

In the present work, we demonstrated that Gal-8-induced antigen internalization and processing is traduced in an incremented peptide-MHC-II complexes presentation to the $CD4^+$ T cells. Remarkably, $CD4^+$ T cell response was not recapitulated using $OVA_{323-339}$ cognate peptide as the antigen source, since it does not require internalization or further degradation, being able to directly accommodate onto MHC-II molecules at the APC surface (Santambrogio et al., 1999). Moreover, an increased antigen presentation was still evident when BMDCs previously pulsed with antigen in the presence of Gal-8 were fixed before the co-culture with $CD4^+$ T cells. Taken together, these results reveal an intrinsic role of Gal-8 in antigen internalization, processing, and presentation that does not depend on its previously reported costimulatory activity of $CD4^+$ T cell response.

Activation of *naive* T helper (Th) cells requires three distinct signals delivered by DC, that integrated, delineate the T cell differentiation process: inflammatory versus tolerogenic (Corthay, 2006). Signal I is delivered by MHC-II in complex with a peptide processed from captured antigens and is received by a specific T cell receptor. Signal II or costimulatory signal is mainly provided by the engagement of CD28 from the TCR complex by CD80 and CD86 molecules on the DCs. This signal is mandatory since TCR signaling in the absence of costimulation renders T cells anergic. Finally, signal III corresponds to soluble factors such as IL-12, IL-15, IL-6, or TNF-α and is also important for functional activation of effector T cells. Notably, Gal-8 reinforces each of the three signals required for the efficient elicitation of primary T cell responses. Regarding the second signal, we have previously reported that this lectin can induce full maturation of both BMDCs as well as splenic DCs, characterized by the upregulation of MHC-II, CD80, and CD86 surface expression (Carabelli et al., 2017). More recently, we demonstrated that endogenous APCs secrete IL-6 in response to Gal-8 stimulation and that cytokine signaling costimulates antigen recognition by cognate $CD4^+$ T cells, thus strengthening the third signal (Carabelli et al., 2018). Here, we demonstrate that Gal-8 is also capable of reinforcing signal I, by enhancing antigen capture, processing, and presentation.

Notwithstanding the general assumption that, when DCs become activated, antigen uptake is negatively regulated, whereas migration and antigen presentation ability are upregulated (Trombetta and Mellman, 2005), there is a time window soon after activation and before migration from tissues to lymphoid organs, in which mature APCs display transient increased antigen internalization (Platt et al., 2010; West et al., 2004). This implies that, at the very beginning of the adaptive immune response, Gal-8 can promote APCs maturation as well as antigen uptake. It has been previously shown that Gal-8 expression is incremented in inflammatory conditions in several tissues and cells (reviewed in Tribulatti et al., 2020), suggesting a role for the endogenous Gal in immune response and inflammation. Endothelial cells from both lymphatic and vascular vessels may constitute an important *in vivo* source for secreted Gal-8 in different peripheral tissues, with the potential to deliver lectin activity to immature APCs (Cattaneo et al., 2014; Cueni and Detmar, 2009; Obino et al., 2018; Stancic et al., 2011; Thijssen et al., 2008). Gal-8 is also found in primary and secondary lymphoid organs, and Gal-8 mRNA was observed specifically in the paracortical T zone area of lymph nodes (Obino et al., 2018; Tribulatti et al., 2007, 2009). It is therefore feasible that endogenous Gal-8 stimulates antigen uptake *in vivo* given its reported localization in APC-antigen encounter sites.

We have previously demonstrated that Gal-8 is expressed by BMDCs at the protein level and that its expression is up-regulated during cell activation (Carabelli et al., 2017). These findings support the notion that endogenous Gal-8 may bind to surface glycans after being secreted by BMDCs, thus acting in an autocrine fashion. In line with this, BMDCs differentiated from *Lgals8*$^{-/-}$ mice displayed impaired capacity to promote antigen-specific CD4^{+} T cell activation (Carabelli et al., 2017). However, in the present work, no differences in antigen internalization or degradation between immature *Lgals8*$^{-/-}$ and WT BMDCs were recorded. It is possible that, to form a lattice structure at the cell surface higher Gal-8 amounts are needed, as those reached with the exogenously added recombinant protein. In this regard, it should be noted that recombinant protein concentration used throughout this work might resemble the endogenous levels reached upon secretion, and remaining attached to the glycoconjugates at the cell surface or the extracellular matrix, in a highly localized manner. BMDCs themselves express increased levels of Gal-8 during activation, further suggesting that high amounts of Gal-8 can be available at the cell membrane particularly during a pro-inflammatory response. Alternatively, the apparent lack of endogenous Gal-8 activity can be explained by the presence of lattices formed by other endogenous Gals members at the APC surface that may cooperate with Gal-8-induced antigen internalization and processing. It has been reported that Gal-1 and Gal-3 are also synthesized by BMDCs at the protein level (Hsu et al., 2009; Ilarregui et al., 2009). Interestingly, Gal-1 is secreted in large amounts by immature BMDCs but, unlike Gal-8, its expression decreased substantially after maturation (Ilarregui et al., 2009). Similar to Gal-8, intracellular Gal-3 expression was found incremented after BMDCs maturation; however, its exposure at the outer membrane was almost marginal despite cellular activation status (Hsu et al., 2009). These observations suggest Gal expression profile in BMDCs is likely to differ upon cell maturation. Since redundant and antagonistic effects among Gal-1, Gal-3, and Gal-8 were observed in other cellular responses when they were simultaneously present (Tribulatti et al., 2012; Weinmann et al., 2018), it would be very interesting to establish in a near future which kind of interactions are taking place among these Gals during antigen uptake and processing on APCs. In any case, the addition of exogenous Gal-8 (even in the absence of the endogenous lectin) was sufficient to induce antigen internalization and processing, as demonstrated in the present work.

Antigen uptake induction constitutes a desirable immunostimulatory property (Reed et al., 2013), actually found among the mechanisms of action of safe and effective approved adjuvants like alum and MF59 (Ghimire et al., 2012; O'Hagan et al., 2012). In the present study, we demonstrated that Gal-8-glycan interaction at the cell surface can stimulate soluble antigen internalization by APCs, leading to a sustained antigen presentation. The adjuvant effect of exogenous Gal-8 has been previously explored by our group using an experimental vaccine model. Co-administration of recombinant Gal-8 and inactivated foot-and-mouth disease virus (FMDV) elicited a major protective antibody-mediated response in BALB/cJ mice, compared with the immunization with only viral antigen (Carabelli et al., 2017). In agreement with our findings, Obino et al. (2018) showed that exogenously added Gal-8 is able to increase the number of antigen-specific germinal center B cells and T follicular helper cells. As a mechanism of action, these authors demonstrated that Gal-8 enhances particulate-antigen acquisition by B cells *in vivo*, promoting its presentation by stabilizing the B-immune synapse and enhancing B cell responses.

In summary, the results presented in this work add to the mechanisms of action of Gal-8 immunostimulatory activity, and at the same time, position this lectin as an integral enhancer of the three required signals for an effective antigen presentation.

Limitations of the Study

This work was conducted using APCs differentiated *in vitro* from GM-CSF conditioned bone marrow cultures (BMDCs), which comprise a heterogeneous population of DCs (GM-DC) and macrophages (GM-M), as previously demonstrated (Carabelli et al., 2017; Helft et al., 2015). Although BMDCs constitute a well-established model that has been largely used to study many aspects of APCs physiology, they might not fully represent the endogenous DCs from an *in vivo* system.

Resource Availability

Lead Contact

Further information and requests should be directed to the Lead Contact, María Virginia Tribulatti (vtribulatti@iib.unsam.edu.ar).

Materials Availability

This study did not generate new unique reagents.

Data and Code Availability

The datasets supporting the current study are available from the corresponding author on request.

METHODS

All methods can be found in the accompanying Transparent Methods supplemental file.

SUPPLEMENTAL INFORMATION

Supplemental Information can be found online at https://doi.org/10.1016/j.isci.2020.101278.

ACKNOWLEDGMENTS

J.C. is fellow and M.V.T. and O.C. are researchers from Consejo Nacional de Investigaciones Científicas y Técnicas (CONICET; Argentina). C.A.P. is fellow from Agencia Nacional de Promoción Científica y Tecnológica (ANPCyT; Argentina). This work was supported by Agencia Nacional de Promoción Científica y Tecnológica (ANPCyT; Argentina) (Grant numbers PICT 2015-2587, PICT 2017-0630).

AUTHORS CONTRIBUTIONS

Conceptualization, C.A.P. and M.V.T.; Methodology, C.A.P., J.C., and M.V.T.; Investigation, C.A.P., J.C., and M.V.T.; Writing – Original Draft, C.A.P. and M.V.T.; Writing – Review & Editing, C.A.P., J.C., O.C., and M.V.T.; Funding Acquisition, O.C. and M.V.T.; Supervision, J.C., O.C., and M.V.T.

DECLARATION OF INTERESTS

The authors declare no competing interests.

Received: March 30, 2020
Revised: May 16, 2020
Accepted: June 12, 2020
Published: June 26, 2020

REFERENCES

Ahmad, S., Zamry, A.A., Tan, H.-T.T., Wong, K.K., Lim, J., and Mohamud, R. (2017). Targeting dendritic cells through gold nanoparticles: a review on the cellular uptake and subsequent immunological properties. Mol. Immunol. *91*, 123–133.

Brewer, C.F. (2002). Thermodynamic binding studies of galectin-1, -3 and -7. Glycoconj. J. *19*, 459–465.

Burgdorf, S., Kautz, A., Bohnert, V., Knolle, P.A., and Kurts, C. (2007). Distinct pathways of antigen uptake and intracellular routing in CD4 and CD8 T cell activation. Science *316*, 612–616.

Burgdorf, S., and Kurts, C. (2008). Endocytosis mechanisms and the cell biology of antigen presentation. Curr. Opin. Immunol. *20*, 89–95.

Carabelli, J., Prato, C.A., Sanmarco, L.M., Aoki, M.P., Campetella, O., and Tribulatti, M.V. (2018). Interleukin-6 signalling mediates Galectin-8 co-stimulatory activity of antigen-specific CD4 T-cell response. Immunology *155*, 379–386.

Carabelli, J., Quattrocchi, V., D'Antuono, A., Zamorano, P., Tribulatti, M.V., and Campetella, O. (2017). Galectin-8 activates dendritic cells and stimulates antigen-specific immune response elicitation. J. Leukoc. Biol. *102*, 1237–1247.

Cárcamo, C., Pardo, E., Oyanadel, C., Bravo-Zehnder, M., Bull, P., Cáceres, M., Martínez, J., Massardo, L., Jacobelli, S., González, A., et al. (2006). Galectin-8 binds specific β1 integrins and induces polarized spreading highlighted by asymmetric lamellipodia in Jurkat T cells. Exp. Cell Res. *312*, 374–386.

Carlsson, S., Oberg, C.T., Carlsson, M.C., Sundin, A., Nilsson, U.J., Smith, D., Cummings, R.D., Almkvist, J., Karlsson, A., and Leffler, H. (2007). Affinity of galectin-8 and its carbohydrate recognition domains for ligands in solution and at the cell surface. Glycobiology *17*, 663–676.

Cattaneo, V., Tribulatti, M.V., and Campetella, O. (2011). Galectin-8 tandem-repeat structure is essential for T-cell proliferation but not for co-stimulation. Biochem. J. *434*, 153–160.

Cattaneo, V., Tribulatti, M.V., Carabelli, J., Carestia, A., Schattner, M., and Campetella, O. (2014). Galectin-8 elicits pro-inflammatory activities in the endothelium. Glycobiology *24*, 966–973.

Coria, L.M., Ibanez, A.E., Tkach, M., Sabbione, F., Bruno, L., Carabajal, M.V., Berguer, P.M., Barrionuevo, P., Schillaci, R., Trevani, A.S., et al. (2016). A Brucella spp. protease inhibitor limits antigen lysosomal proteolysis, increases cross-presentation, and enhances CD8+ T cell responses. J. Immunol. *196*, 4014–4029.

Corthay, A. (2006). A three-cell model for activation of naive T helper cells. Scand. J. Immunol. *64*, 93–96.

Cueni, L.N., and Detmar, M. (2009). Galectin-8 interacts with podoplanin and modulates lymphatic endothelial cell functions. Exp. Cell Res. *315*, 1715–1723.

Elola, M.T., Wolfenstein-Todel, C., Troncoso, M.F., Vasta, G.R., and Rabinovich, G.A. (2007). Galectins: matricellular glycan-binding proteins linking cell adhesion, migration, and survival. Cell Mol. Life Sci. *64*, 1679–1700.

Eshkar Sebban, L., Ronen, D., Levartovsky, D., Elkayam, O., Caspi, D., Aamar, S., Amital, H., Rubinow, A., Golan, I., Naor, D., et al. (2007). The involvement of CD44 and its novel ligand galectin-8 in apoptotic regulation of autoimmune inflammation. J. Immunol. *179*, 1225–1235.

Franken, L., Kurts, C., and Burgdorf, S. (2013). Monitoring the intracellular routing of internalized antigens by immunofluorescence microscopy. In Antigen Processing: Methods and Protocols, P. van Endert, ed. (Humana Press), pp. 371–377.

Furtak, V., Hatcher, F., and Ochieng, J. (2001). Galectin-3 mediates the endocytosis of beta-1 integrins by breast carcinoma cells. Biochem. Biophys. Res. Commun. *289*, 845–850.

Ghimire, T.R., Benson, R.A., Garside, P., and Brewer, J.M. (2012). Alum increases antigen uptake, reduces antigen degradation and sustains antigen presentation by DCs in vitro. Immunol. Lett. *147*, 55–62.

Helft, J., Böttcher, J., Chakravarty, P., Zelenay, S., Huotari, J., Schraml, B.U., Goubau, D., and Reis e Sousa, C. (2015). GM-CSF mouse bone marrow cultures comprise a heterogeneous population of CD11c(+)MHCII(+) macrophages and dendritic cells. Immunity *42*, 1197–1211.

Holland, J.W. (2008). Chapter 4 - post-translational modifications of caseins. In Milk Proteins, A. Thompson, M. Boland, and H. Singh, eds. (Academic Press), pp. 107–132.

Hsu, D.K., Chernyavsky, A.I., Chen, H.-Y., Yu, L., Grando, S.A., and Liu, F.-T. (2009). Endogenous galectin-3 is localized in membrane lipid rafts and regulates migration of dendritic cells. J. Invest. Dermatol. *129*, 573–583.

Ilarregui, J.M., Croci, D.O., Bianco, G.A., Toscano, M.A., Salatino, M., Vermeulen, M.E., Geffner, J.R., and Rabinovich, G.A. (2009). Tolerogenic signals delivered by dendritic cells to T cells through a galectin-1-driven immunoregulatory circuit involving interleukin 27 and interleukin 10. Nat. Immunol. *10*, 981–991.

Johannes, L., Jacob, R., and Leffler, H. (2018). Galectins at a glance. J. Cell Sci. *131*, jcs208884.

Kim, S.J., Schatzle, S., Ahmed, S.S., Haap, W., Jang, S.H., Gregersen, P.K., Georgiou, G., and Diamond, B. (2017). Increased cathepsin S in Prdm1(-/-) dendritic cells alters the TFH cell repertoire and contributes to lupus. Nat. Immunol. *18*, 1016–1024.

Lakshminarayan, R., Wunder, C., Becken, U., Howes, M.T., Benzing, C., Arumugam, S., Sales, S., Ariotti, N., Chambon, V., Lamaze, C., et al. (2014). Galectin-3 drives glycosphingolipid-dependent biogenesis of clathrin-independent carriers. Nat. Cell Biol. *16*, 595–606.

Lepur, A., Carlsson, M.C., Novak, R., Dumic, J., Nilsson, U.J., and Leffler, H. (2012). Galectin-3 endocytosis by carbohydrate independent and dependent pathways in different macrophage like cell types. Biochim. Biophys. Acta *1820*, 804–818.

Levy, Y., Arbel-Goren, R., Hadari, Y.R., Eshhar, S., Ronen, D., Elhanany, E., Geiger, B., and Zick, Y. (2001). Galectin-8 functions as a matricellular modulator of cell adhesion. J. Biol. Chem. *276*, 31285–31295.

Liu, F.T., and Rabinovich, G.A. (2010). Galectins: regulators of acute and chronic inflammation. Ann. N. Y. Acad. Sci. *1183*, 158–182.

Lutz, M.B., Rovere, P., Kleijmeer, M.J., Rescigno, M., Assmann, C.U., Oorschot, V.M., Geuze, H.J., Trucy, J., Demandolx, D., Davoust, J., et al. (1997). Intracellular routes and selective retention of antigens in mildly acidic cathepsin D/lysosome-associated membrane protein-1/MHC class II-positive vesicles in immature dendritic cells. J. Immunol. *159*, 3707–3716.

Martínez Allo, V.C., Toscano, M.A., Pinto, N., and Rabinovich, G.A. (2018). Galectins: key players at the frontiers of innate and adaptive immunity. Trends Glycosci. Glycotechnol. *30*, SE97–SE107.

Mathew, M.P., and Donaldson, J.G. (2018). Distinct cargo-specific response landscapes underpin the complex and nuanced role of galectin-glycan interactions in clathrin-independent endocytosis. J. Biol. Chem. *293*, 7222–7237.

Mathew, M.P., and Donaldson, J.G. (2019). Glycosylation and glycan interactions can serve as extracellular machinery facilitating clathrin-independent endocytosis. Traffic *20*, 295–300.

Mellman, I., and Steinman, R.M. (2001). Dendritic cells: specialized and regulated antigen processing machines. Cell *106*, 255–258.

O'Hagan, D.T., Ott, G.S., De Gregorio, E., and Seubert, A. (2012). The mechanism of action of MF59 - an innately attractive adjuvant formulation. Vaccine *30*, 4341–4348.

Obino, D., Fetler, L., Soza, A., Malbec, O., Saez, J.J., Labarca, M., Oyanadel, C., Del Valle Batalla, F., Goles, N., Chikina, A., et al. (2018). Galectin-8 favors the presentation of surface-tethered antigens by stabilizing the B cell immune synapse. Cell Rep. *25*, 3110–3122.e6.

Olatunde, A.C., Abell, L.P., Landuyt, A.E., and Hiltbold Schwartz, E. (2018). Development of endocytosis, degradative activity, and antigen processing capacity during GM-CSF driven differentiation of murine bone marrow. PLoS One *13*, e0196591.

Platt, C.D., Ma, J.K., Chalouni, C., Ebersold, M., Bou-Reslan, H., Carano, R.A.D., Mellman, I., and Delamarre, L. (2010). Mature dendritic cells use endocytic receptors to capture and present antigens. Proc. Natl. Acad. Sci. U S A *107*, 4287–4292.

Reed, S.G., Orr, M.T., and Fox, C.B. (2013). Key roles of adjuvants in modern vaccines. Nat. Med. *19*, 1597–1608.

Renard, H.-F., Tyckaert, F., Lo Giudice, C., Hirsch, T., Valades-Cruz, C.A., Lemaigre, C., Shafaq-Zadah, M., Wunder, C., Wattiez, R., Johannes, L., et al. (2020). Endophilin-A3 and Galectin-8 control the clathrin-independent endocytosis of CD166. Nat. Commun. *11*, 1457.

Santambrogio, L., Sato, A.K., Carven, G.J., Belyanskaya, S.L., Strominger, J.L., and Stern, L.J. (1999). Extracellular antigen processing and presentation by immature dendritic cells. Proc. Natl. Acad. Sci. U S A *96*, 15056–15061.

Schroeder, M.N., Tribulatti, M.V., Carabelli, J., Andre-Leroux, G., Caramelo, J.J., Cattaneo, V., and Campetella, O. (2016). Characterization of a double-CRD-mutated Gal-8 recombinant protein that retains co-stimulatory activity on antigen-specific T-cell response. Biochem. J. *473*, 887–898.

Stancic, M., van Horssen, J., Thijssen, V.L., Gabius, H.J., van der Valk, P., Hoekstra, D., and Baron, W. (2011). Increased expression of distinct galectins in multiple sclerosis lesions. Neuropathol. Appl. Neurobiol. *37*, 654–671.

Steinman, R.M. (2006). Linking innate to adaptive immunity through dendritic cells. Novartis Found. Symp. *279*, 101–109, discussion: 109–13, 216–9.

Stowell, S.R., Arthur, C.M., Slanina, K.A., Horton, J.R., Smith, D.F., and Cummings, R.D. (2008). Dimeric Galectin-8 induces phosphatidylserine exposure in leukocytes through polylactosamine recognition by the C-terminal domain. J. Biol. Chem. *283*, 20547–20559.

Thijssen, V.L., Hulsmans, S., and Griffioen, A.W. (2008). The galectin profile of the endothelium: altered expression and localization in activated and tumor endothelial cells. Am. J. Pathol. *172*, 545–553.

Tribulatti, M.V., Carabelli, J., Prato, C.A., and Campetella, O. (2020). Galectin-8 in the onset of the immune response and inflammation. Glycobiology *30*, 134–142.

Tribulatti, M.V., Cattaneo, V., Hellman, U., Mucci, J., and Campetella, O. (2009). Galectin-8 provides costimulatory and proliferative signals to T lymphocytes. J. Leukoc. Biol. *86*, 371–380.

Tribulatti, M.V., Figini, M.G., Carabelli, J., Cattaneo, V., and Campetella, O. (2012). Redundant and antagonistic functions of galectin-1, -3, and -8 in the elicitation of T cell responses. J. Immunol. *188*, 2991–2999.

Tribulatti, M.V., Mucci, J., Cattaneo, V., Aguero, F., Gilmartin, T., Head, S.R., and Campetella, O. (2007). Galectin-8 induces apoptosis in the CD4(high)CD8(high) thymocyte subpopulation. Glycobiology *17*, 1404–1412.

Trombetta, E.S., and Mellman, I. (2005). Cell biology of antigen processing in vitro and in vivo. Annu. Rev. Immunol. *23*, 975–1028.

Weinmann, D., Kenn, M., Schmidt, S., Schmidt, K., Walzer, S.M., Kubista, B., Windhager, R., Schreiner, W., Toegel, S., and Gabius, H.J. (2018). Galectin-8 induces functional disease markers in human osteoarthritis and cooperates with galectins-1 and -3. Cell Mol. Life Sci. *75*, 4187–4205.

West, M.A., Wallin, R.P., Matthews, S.P., Svensson, H.G., Zaru, R., Ljunggren, H.G., Prescott, A.R., and Watts, C. (2004). Enhanced dendritic cell antigen capture via toll-like receptor-induced actin remodeling. Science *305*, 1153–1157.

Zappelli, C., van der Zwaan, C., Thijssen-Timmer, D.C., Mertens, K., and Meijer, A.B. (2012). Novel role for galectin-8 protein as mediator of coagulation factor V endocytosis by megakaryocytes. J. Biol. Chem. *287*, 8327–8335.

iScience, Volume *23*

Supplemental Information

Galectin-8 Enhances T cell Response by Promotion of Antigen Internalization and Processing

Cecilia Arahí Prato, Julieta Carabelli, Oscar Campetella, and María Virginia Tribulatti

SUPPLEMENTAL FIGURES

Figure S1

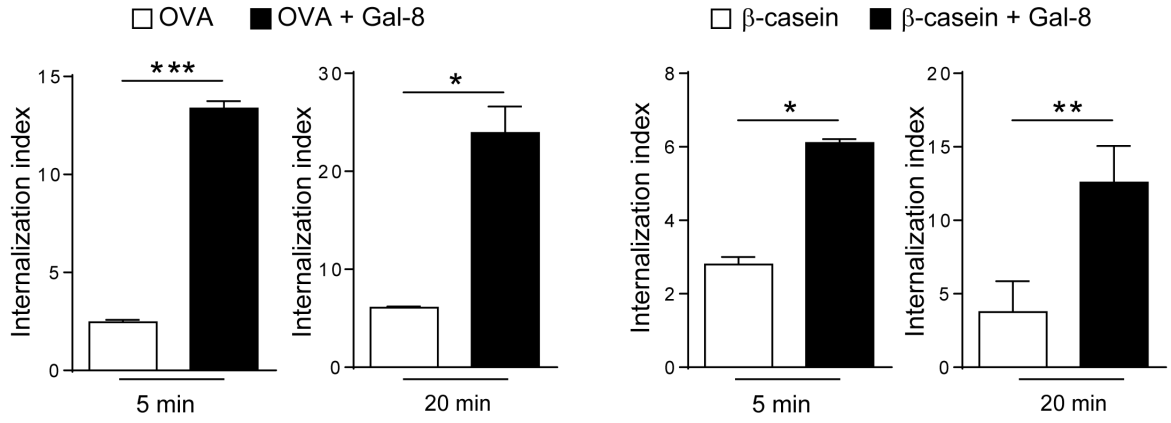

Figure S1. Gal-8 increases β-casein and OVA internalization in BMDCs, Related to Figure 2. (**A**) BMDCs were incubated at 37°C for the indicated time points with 50 μg/ml Alexa 488-OVA or 50 μg/ml biotin-β-casein with the simultaneous addition of 2 μM Gal-8. Then, the internalization index was calculated as the ratio between the mean of fluorescence of treated and control cells. *p<0.05, **p<0.01, ***p<0.001 (*t* test). Depicted assays are representative of at least two independent experiments.

Figure S2

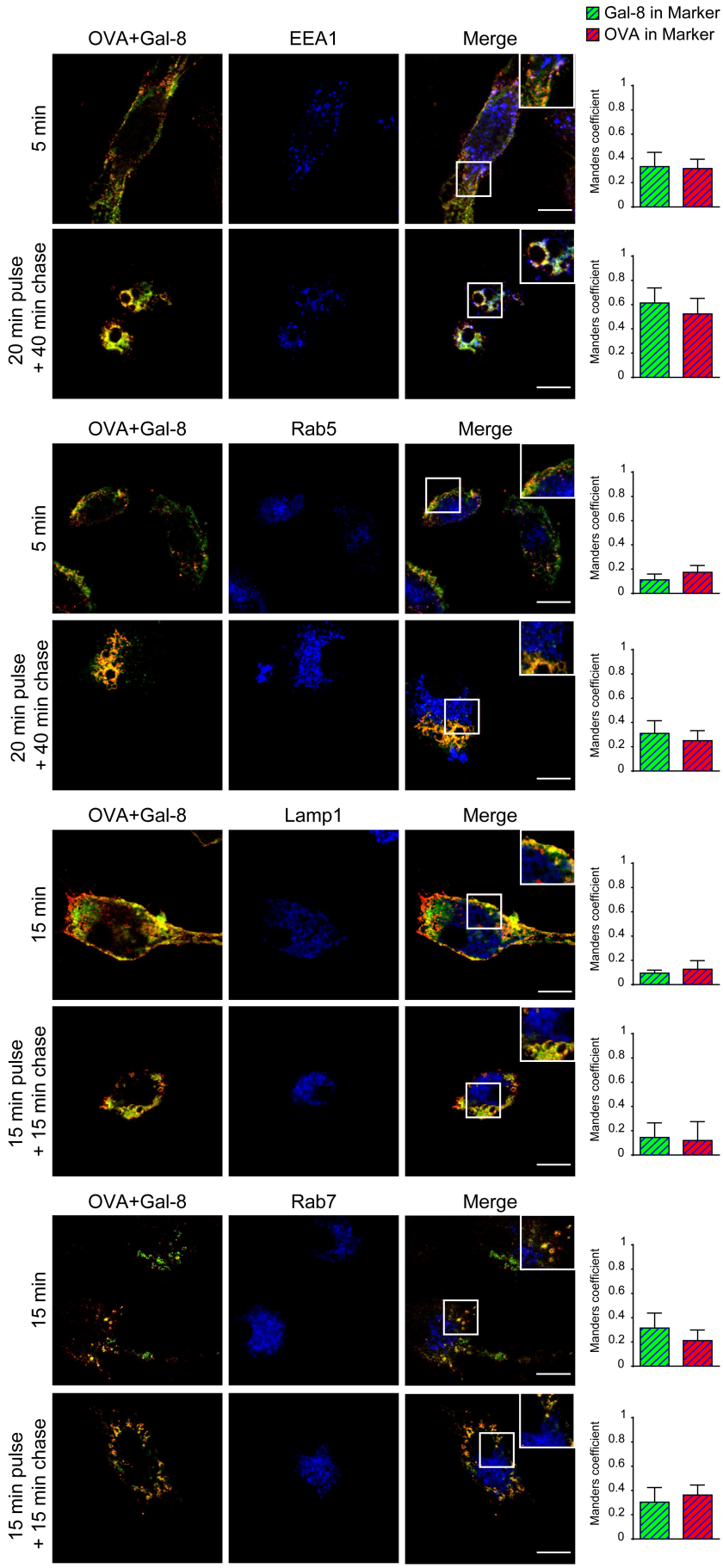
Gal-8 in Marker
OVA in Marker
OVA+Gal-8
EEA1
Merge
5 min
20 min pulse
+ 40 min chase
Manders coefficient
OVA+Gal-8
Rab5
Merge
5 min
20 min pulse
+ 40 min chase
Manders coefficient
OVA+Gal-8
Lamp1
Merge
15 min
15 min pulse
+ 15 min chase
Manders coefficient
OVA+Gal-8
Rab7
Merge
15 min
15 min pulse
+ 15 min chase
Manders coefficient

Figure S2. Subcellular localization of internalized Gal-8 and OVA antigen, Related to Figure 3. BMDCs were incubated with 50 μg/ml Alexa 488-OVA and 0.2 μM of Alexa 568Gal-8 plus 1.8 μM of unlabeled Gal-8 for the indicated times, then cells were fixed, permeabilized, and stained with anti-EEA1, -Rab5, -Lamp1 and -Rab7. Quantification of colocalization of Gal-8 signal in Marker signal and OVA signal in Marker signal was analyzed with Manders' overlap coefficient. Representative images from confocal microscopy are shown. Manders' coefficients were calculated using the JACOP plugin on FIJI setting the threshold manually. Scale bar: 10 μm. Bars represent the mean ± SD of Manders coefficient from 10 fields containing at least two cells per field.

Figure S3

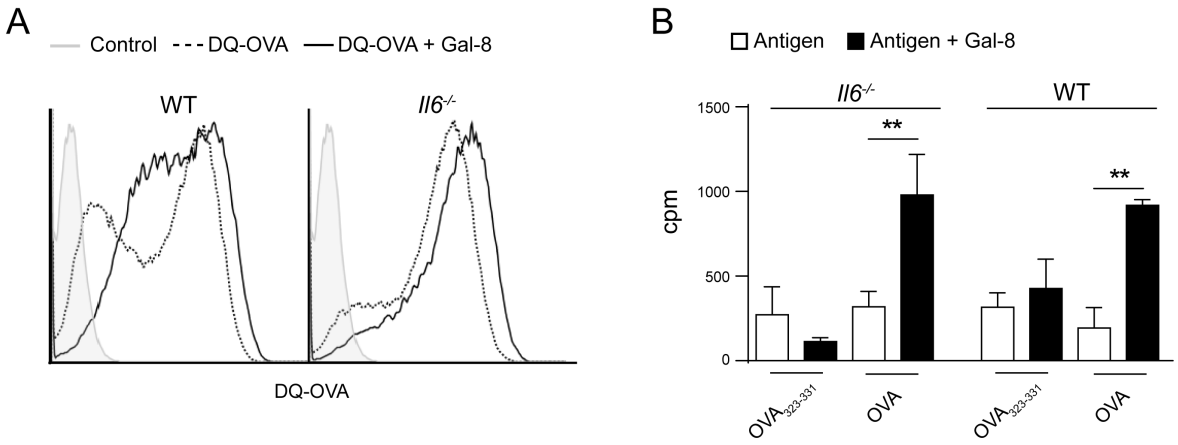

Figure S3. Gal-8-induced antigen processing and presentation are not affected in IL-6-deficient BMDCs, Related to Figure 5. (**A**) BMDCs differentiated from *Il6*$^{-/-}$ or C57BL/6J (WT) mice were pulsed with 50 µg/ml DQ-OVA and 2 µM Gal-8 for 15 min at 37°C, washed and chased for 45 min. Fluorescence emitted by DQ-OVA was analyzed by flow cytometry. (**B**) BMDCs differentiated from *Il6*$^{-/-}$ or C57BL/6J (WT) mice were pulsed with 0.1 µg/ml OVA peptide ($OVA_{323-339}$) or 1 mg/ml OVA protein (OVA) in the presence of Gal-8 for 18h at 37°C. Then, cells were washed, fixed, and co-incubated with $CD4^+$ T cells purified from OT-II mice splenocytes for 72 h. Cell proliferation was assessed by [^{3}H]-methyl-thymidine incorporation. **p<0.01 (*t* test).

TRANSPARENT METHODS

Mice and cell lines

BALB/cJ, C57BL/6J, OT-II [B6.Cg-Tg(TcraTcrb)425Cbn/J] and B6.129S2-*Il6*^{tm1Kopf}/J (*Il6*$^{-/-}$) breeding pairs were obtained from The Jackson Laboratory (Bar Harbor, ME) and bred in our facilities. Mice knockout for the Gal-8 coding sequence gene (*Lgals8*$^{-/-}$) [B6;129S5-Lgals8 /Mmucd] were obtained from Mutant Mouse Resource & Research Centers (MMRRC; University of California, Davis, CA, USA) as heterozygous. After in-house 12 backcrosses to C57BL/6J, a homozygous knockout colony with 95% of the C57BL/6J genetic background was established, as assessed at The Jackson Laboratory Genotyping Resources. The Ethics Committee Board of the Universidad Nacional de San Martín approved all procedures involving animals. Immortalized murine macrophage-like J774 A.1 cell line (ATCC® TIB-67™) was maintained by weekly passages in RPMI 1640 (Gibco, ThermoFisher Scientific, Waltham, MA), supplemented with 10% fetal bovine serum (Gibco) at 37°C and 5% CO_2.

Reagents

For DC phenotyping, fluorochrome-conjugated anti-CD11c (clone: M1/70), anti-MHC-II (clone: M5/114.15.2), anti-CD80 (clone: PO3) and anti-CD86 (clone: 1610A1) mAbs were used (BioLegend). Anti-EEA1 (clone: C45B10) and anti-Rab5 (clone: C8B1) mAbs were obtained from Cell Signaling Technology. Anti-Rab7 (clone: W16034A) and Alexa 647 anti-Lamp1 (clone: 1D4B) mAbs, Alexa 647anti-rabbit (Poly4064) and anti-rat (Poly4054) immunoglobulins secondary polyclonal antibodies, and PE/Cy5-conjugated streptavidin were all obtained from Biolegend. For ELISA, biotin anti-mouse IFN-γ (clone: XMG1.2), purified anti-mouse IFN-γ (clone: R4-6A2), biotin anti-mouse IL-6 (clone: MP5-32C11) and purified anti-mouse IL-6 (clone: MP5-20F3) antibodies were used (all from BioLegend).

Recombinant Gals

To obtain recombinant Gal-8, mouse Gal-8L isoform (GenBank: EF524570) was cloned by PCR using cDNA as a template, obtained from thymocytes mRNA by retrotranscription (Tribulatti et al., 2007). The amplified open reading frame was cloned into pTrcHis B (Invitrogen) expression plasmid and transformed into *Escherichia coli* BL-21. Overnight cultures were diluted 1/100 in 500 mL of Terrific Broth (USB Bio) plus ampicillin, and incubated with agitation at 37°C. At

OD600nm=1, 0.5mM isopropyl-ß-D-thio galactopyranoside (Sigma-Aldrich, St Louis, MO) was added and the culture was incubated for 18 h at 18°C with agitation. The pellet was resuspended in 30 mL of buffer 1X PBS containing 0.5% Triton X-100, 2 mM EDTA and 1 mM phenylmethylsulfonyl fluoride (PMSF), pH 7.4, and lysed by sonication. Cell debris was removed by centrifugation at 4°C. The soluble extract were filtered through a 0.45 µm pore membrane and seeded into a 1mL Lactosyl-Sepharose column (Sigma-Aldrich). After washing with twenty volumes of 1X PBS, the lectin was eluted with 10 mL of 1X PBS plus 100 mM lactose (Sigma-Aldrich) and 1mM PMSF. Then, protein eluate was diluted in equilibration buffer (20 mM Tris–HCl pH 8.8, 500 mM NaCl, 30 mM imidazole), and seeded into a previously equilibrated 1 mL His-Trap Column, (GE-Healthcare, Uppsala, Sweden). After washing the column with ten volumes of equilibration buffer, Gal-8 was eluted with 20 mM Tris-HCl pH 6.8, 500 mM NaCl, 100 mM imidazole. About 3–5 mg of pure recombinant lectins were recovered by this protocol. Gal-8mut was designed by replacing two key arginine residues (Arg_{68}His and Arg_{241}His) from mouse Gal-8L isoform in a synthetic gene construction (Genscript). For protein expression, the same conditions described previously for Gal-8 were followed, except for purification, where two consecutive rounds of immobilized metal-affinity chromatography were performed, owing to the lack of lactose-binding capacity of the mutated protein. Purity was checked by 10% SDS-PAGE, and protein concentration was assessed using NanoDrop (UV-Vis ThermoScientific™ NanoDrop™ One). Proteins were dialyzed overnight against 2 L of 50 mM Tris–HCl pH 7.6, 500 mM NaCl. Then 10% (v/v) glycerol (Sigma-Aldrich) were added to stabilize recombinant Gals preparations. Endotoxins were eliminated using Pierce High-Capacity Endotoxin removal resin (ThermoFisher Scientific) following manufacturer's instructions, resulting in less than 0.1 endotoxin units per milligram of protein. Lectin activity was tested by haemagglutination assay. Briefly, 50 µL of a 4% v/v suspension of PBS-washed fresh mouse red blood cells (RBC) were mixed with 50 µL of two-fold serial dilutions of the recombinant Gals in 1X PBS plus 2% BSA. The reaction was performed in a 96-round bottom well plate and incubated for 1 h at room temperature.

Protein labeling

Alexa-labeled proteins were prepared according to the manufacturer's instructions (Protein labeling Kit, Molecular Probes, ThermoFisher Scientific). Briefly, 1 mg of Gal-8 or chicken egg ovalbumin (OVA, Grade V, Sigma-Aldrich) was incubated with the corresponding dye and then labeled protein was purified on a molecular exclusion column. Recovered protein concentration and labeling degree were quantified using NanoDrop. Biotin-OVA and biotin-β-casein were prepared according to manufacturer´s instructions using EZ-Link NHS- Biotin (Molecular Probes). Briefly, 1 mg of OVA or β-casein (Sigma-Aldrich) was mixed with 10 mM biotin reagent solution

and incubated on ice for 2 hours. Proteins were dialyzed overnight against 1X PBS, to remove the excess of non-reacted and hydrolyzed biotin reagent.

BMDCs

Bone marrow (BM) was obtained from femurs and tibias from 6- to 10-wk-old male mice by flushing RPMI 1640 medium through the bone interior. The cell suspension was washed and RBC were lysed with RBC lysis buffer (Sigma-Aldrich). Then, cells were cultured at 37°C and 5% CO_2 in six-well plates (1.5 x 10^6 cells per well) in 2 ml RPMI 1640 containing 10% FBS, 50 µg/ml Gentamycin (Sigma-Aldrich) and 20 ng/ml of recombinant GM-CSF (GenScript). Media was renovated on days 3 and 5, then cells were harvested on day 8 and the expression of DC (CD11c, MHC-II) and activation (CD86 and CD80) markers were analyzed by flow cytometry.

Gal internalization and subcellular localization

BMDCs ($2x10^5$) differentiated from BALB/cJ males were incubated for different periods with 0.2 µM Alexa 568-Gal-8 plus 1.8 µM of unlabeled Gal-8 alone, or in combination with Alexa 488-OVA when indicated, at 37°C and 5% CO_2 for internalization, or on ice for surface binding analysis. Then, cells were washed with ice-cold PBS and fixed with 2% paraformaldehyde (PFA, EM Grade) for 10 min. For intracellular immunostaining, cells were permeabilized and blocked for 1 h in 0.5% saponin, 3% BSA, 1X PBS solution, and then incubated for 18 h at 4°C on a humid chamber with one of the following primary antibodies in 0.1% saponin, 1% BSA, 1X PBS solution: anti-EEA1 (1:500), anti-Rab5 (1:200), anti-Rab7 (1:200) and anti-Lamp1 (1:600), followed by 1 h incubation at room temperature with secondary antibodies. Cells were mounted in fluorescent mounting medium (FluorSave, MerckMillipore) before observation with an Olympus FV1000 confocal microscope. Images were acquired at a 60 X objective lens with a numeric aperture of 1.42 and 4 µs/pix of dwell time. We manually adjusted the laser energy setting (HV, gain and offset) by using slides stained only with the secondary antibodies to determine the threshold of background signal, which was applied to each image of the experiment. The colocalization analysis was performed using the JACOP plugin on FIJI software.

Gal binding

BMDCs ($2x10^5$) differentiated from BALB/cJ males were resuspended in 100 µl of ice-cold PBS containing sodium azide and treated with 0.1 µM Alexa 488-Gal-8 on ice for 20 min. Then, cells were washed with ice-cold PBS or PBS plus 100 mM lactose, and the fluorescence signal was analyzed by flow cytometry. Cell samples processed without recombinant Gal were included as a negative control.

Antigen binding and internalization

BMDCs ($5x10^5$) differentiated from BALB/cJ males were incubated for the indicated periods in the presence of antigen (50 µg/ml Alexa 488-OVA or biotin-β-casein), at 37°C and 5% CO_2 for internalization, or on ice for surface binding, with or without 2 µM Gal-8. For intracellular biotin-β-casein visualization, cells were washed with ice-cold PBS and fixed and permeabilized with Cytofix/Cytoperm Fixation/Permeabilization Solution (BD, Franklin Lakes, NJ) for 20 min at 4°C. Then cells were stained with 1:1000 PE-Cy5-streptavidin. For surface-bound biotin-β-casein visualization, cells were stained as before, but without permeabilization. Then, cells were washed with ice-cold PBS containing sodium azide and analyzed by flow cytometry. When indicated, PBS plus 100 mM lactose was added. Cell samples processed without antigen were included as a negative control. For antigen binding analysis by confocal microscopy, $2x10^5$ BMDCs were incubated with Alexa 488-OVA in the presence of 2 µM of unlabeled Gal-8 for 15 min on ice. When indicated, PBS plus 100 mM lactose was added. Then, cells were washed with ice-cold PBS and fixed with 2% PFA for 10 min. Images were acquired by confocal microscopy as mention previously.

Pull-down assay

Protein A sepharose (30 µl, Pharmacia Biotech) were incubated with 4 µg of homemade rabbit affinity-purified anti-mouse Gal-8 polyclonal antibody or normal rabbit IgG (control), for 2 h at 4°C under end-over-end rotation. Then, the resin was washed and incubated with a mix of 20 µg/ml OVA and 0.2 µM Gal-8, (or with only OVA or Gal-8 as controls) for 18 h at 4°C under rotation. Then, samples were washed and eluted with PBS plus 200 mM lactose. Eluates (for lectin-glycan interaction) and resins (for protein-protein interaction) were cracked and solved in a 10% SDS-PAGE before transferred to nitrocellulose membranes. Blots were probed with anti-Gal-8 polyclonal antibody 1/200, and mouse monoclonal anti-OVA antibody 1/2000 (MAbia labs,

Buenos Aires, Argentina), followed by goat anti-rabbit IgG IRDye 680LT and goat anti-mouse IgG IRDye 800CW 1/15000 (both from LI-COR Biosciences), and the infrared signals were captured with LI-COR Odyssey® scanner and software (LI-COR Biosciences).

Antigen processing

BMDCs ($5x10^5$) differentiated from BALB/cJ males were incubated with 50 µg/ml DQ-OVA (ThermoFisher Scientific) for the indicated periods at 37°C and 5% CO_2. After Gal-8-treatment, cells were washed and analyzed by flow cytometry. For simultaneous antigen internalization and processing assay, cells were incubated with 50 µg/ml DQ-OVA together with 50 µg/ml biotin-OVA. After incubation, cells were washed with ice-cold PBS and fixed and permeabilized with Cytofix/Cytoperm Fixation/Permeabilization Solution (BD) for 20 min at 4°C. For intracellular biotin-OVA visualization cells were stained with 1:1000 PE-Cy5-streptavidin. Cells were washed and analyzed by flow cytometry.

Presentation assays

For mouse splenocyte purification, spleens from 6– to 8-wk-old male mice were removed and disrupted against a stainless steel mesh in RPMI 1640 medium. Cell suspension was washed, then RBC were lysed with RBC lysis buffer and cells were washed again with medium. For $CD4^+$ T cell purification, a MojoSort Mouse CD4 Naive Cell Untouched Isolation Kit (BioLegend) was used, following the manufacturer's instructions. Cell purity (>90%) was checked by flow cytometry, after cell staining with anti-CD4 mAb (clone: GK1.5, BioLegend). BMDCs (10^4) from C57BL/6J males were cultured in a 96-round bottom well plate with 100 µl RPMI 1640 containing 10% FBS, 50 µg/ml Gentamycin in the presence of the cognate ovalbumin 323-339 ($OVA_{323–339}$) peptide (Genscript, Piscataway, NJ) or EndoGrade® Endotoxin-free Ovalbumin (Hygloss, Bernried am Starnberger See, Germany) at the indicated concentrations, plus 2 µM Gal-8 during 45 min at 37°C and 5% CO_2. For fixed BMDCs assays, cells were washed afther the pulse with ice-cold PBS, fixed for 1 min on ice-cold glutaraldehyde (0.03% in PBS:RPMI 1:1), and quenched with glycine (100 mM in PBS:RPMI 1:1). Then, cells were washed several times with ice-cold PBS and co-cultured with 10^5 $CD4^+$ T cells purified from OT-II mice for 72 h in a final volume of 200 µl RPMI 1640 containing 10% FBS and 50 µg/ml Gentamycin. Eighteen hours before harvest, 1 µCi [^{3}H]-methyl thymidine (PerkinElmer) was added to each well. Values in cpm were registered in a scintillation counter. For CFSE dilution, $CD4^+$ T cells were previously labeled with CFDA SE (CFSE, Invitrogen), following manufacturer's instructions. Briefly, $CD4^+$ T cells ($2×10^6$ cells/ml) were mixed with the

same volume of 5 μM CFSE in PBS and incubated for 15 min at 37°C. Subsequently, the reaction was stopped by adding FBS at a final concentration of 10% and washed twice with PBS for colorant excess removal. BMDCs and $CD4^+$ T cells were co-cultured for 6 days until flow cytometry analysis. Proliferation assays were performed in quadruplicate.

Cytokine analysis

IFN-γ levels were quantified by commercial ELISA antibodies (BioLegend) in supernatants from antigen presentation assay, following the manufacturer's instructions and using recombinant cytokine–standard curve.

Flow cytometry

FlowMax cytometer PASIII (Partec, Münster, Germany) and Flowjo software (FlowJo, Ashland, OR, USA) were used.

Statistical analysis

Statistical analyses and graphs were performed with GraphPad Prism 6.0. Student's *t* test was used, except for the analysis shown in Fig 4D, where ordinary one-way ANOVA was performed. In all cases, P values < 0.05 were considered significant.